

Charge-radius changes in even- A platinum nuclei

J. K. P. Lee, G. Savard,* J. E. Crawford, and G. Thekkadath
Foster Radiation Laboratory, McGill University, Montréal, Canada

H. T. Duong, J. Pinard, and S. Liberman
Laboratoire Aimé Cotton, Centre National de la Recherche Scientifique II, Orsay, France

F. Le Blanc, P. Kilcher, J. Obert, J. Oms, J. C. Putaux,
 B. Roussière, and J. Sauvage
Institut de Physique Nucléaire, Orsay, France

(Received 13 July 1988)

Isotope shift measurements on even- A Pt isotopes have been obtained from $A=186$ to $A=198$. Charge radius differences have been extracted, and are compared to constrained Hartree-Fock plus BCS calculations. A possible shape transition between ^{186}Pt and ^{188}Pt is discussed.

Laser spectroscopy of long isotopic chains is a very useful tool to study the properties of isomeric or ground-state nuclei, enabling the measurements of the spin and moments of nuclei through the hyperfine structure (HFS) and of the changes in charge radii through the isotopic shift (IS). One of the spectacular early results of optical spectroscopy of radioactive atoms was the observation of a large increase in the mean-square charge radius of mercury isotopes between $A=186$ and $A=185$.¹ This result was later interpreted as a shape transition from a weakly oblate to a well-deformed prolate shape.² The existence of a well-deformed nuclear ground state so close to the magic proton number $Z=82$ generated wide interest. Recently, nuclear spectroscopy results have shown that the $I=3$ ground state of ^{186}Au , due to the $\pi h_{9/2} \nu 9/2^+ [624]$ configuration, corresponds to a prolate-shaped nucleus³ whereas the positive-parity low-spin states of odd- A gold isotopes very likely correspond to oblate-shaped nuclei.⁴ This suggested an oblate to prolate ground-state shape transition in gold isotopes between $A=187$ and $A=186$, which has been confirmed by laser resonance ionization spectroscopy (RIS) measurements.^{5,6} Similar shape transitions and related shape coexistence are also expected to exist in the platinum isotopes. In the even- A case, the level structures of the isotopes with $A \geq 192$ are consistent with a weakly oblate shape, like that of the neighboring Hg and Os isotones. In the lighter isotopes, the systematic study of the nuclear excited states shows a crossing of the 4_1^+ and 2_2^+ states between $A=188$ and $A=186$,⁷ which was interpreted by Kumar⁸ as the signature of an oblate to prolate shape transition. Moreover, the 0_2^+ excited state drops to low energy in the even- A platinum isotopes⁷ with $A \leq 186$; this may be interpreted as a sign of shape coexistence.⁹⁻¹¹

In a discussion of shape coexistence in platinum, Wood^{10,12} has emphasized the role played by the $\pi(h_{9/2})$ orbital in the deformation of the ground and excited states. Near $N=104$, this orbital falls so low in energy that the main component of the 0^+ ground state is $\pi(2p-6h)$, rather than the "normal" $4h$ configuration. Thus, shape transitions may be expected near those regions

where the two 0^+ states are very close; i.e., the ground-state transition would be expected to occur just above $A=186$ for the Pt isotopes.⁷ Near $A=186$, this picture of a shape transition is further supported by the successful interpretation of the level structure of ^{185}Pt as a single neutron coupled to a prolate core.¹³ However, for ^{187}Pt , shape coexistence seems to be present at low energy¹⁴⁻¹⁷ and the ground-state shape is still an open question. The general trend of this transition is explained by various theoretical calculations; these indicate a prolate ground-state shape around $A=182$ and an oblate shape for $A \geq 194$. The exact location of the shape transition has not, however, been pinpointed. In this paper, we report the first laser spectroscopy work on the radioactive Pt isotopes.

Radioactive Au isotopes are produced by (p, xn) reactions on a Pt-B molten target inside the ISOCELE mass-separator ion source. The neutron deficient Pt isotopes are obtained from the radioactive decay of the Au nuclei. The stable Pt isotopes are directly available from the same source. The apparatus in this experiment (Fig. 1) is similar to the one used for a previous study of neutron deficient Au isotopes.^{6,18} The use of pulsed laser desorption to generate a pulsed atomic beam synchronized to the ionizing laser pulses results in a large increase in sensitivity over the previous RIS applications on continuous atomic beams. In addition, a major improvement over the set-up used for the Au study is achieved here in decelerating the ion beam before implantation. The ions are then implanted much closer to the surface enabling the laser desorption to take place at lower heating laser energy density. This results in a reduction of the background due to ions created directly by the heating laser and better reproducibility of the heating conditions.

The energy of the Au ion beam is reduced from 45 keV to about 0.5 keV in a decelerating lens before implantation on a thin graphite sheet over a horizontal line of 2 by 8 mm. The implantation lasts up to one half-life of the daughter Pt nucleus. The graphite sheet is mounted on an insulating tape transport system which moves the implanted sample from the high-voltage decelerating region to the

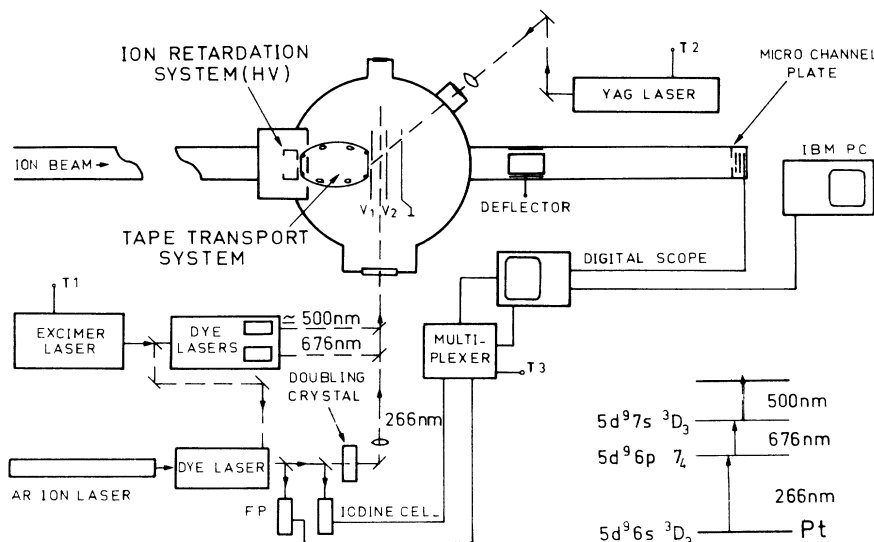


FIG. 1. Experimental setup. FP: Fabry-Perot interferometer; T1, T2, and T3; timing inputs for synchronized operation. The inset shows the Pt atomic levels and transitions chosen for the measurements.

input of an electrostatic time-of-flight (TOF) system. The tape is then moved slowly while a pulsed Nd:Yag laser beam, focused to a vertical line of 2 by 0.05 mm, is fired at the repetition rate of 10 Hz to desorb the implanted atoms and form a pulsed atomic beam. An ensemble of three synchronized dye lasers is then fired to selectively ionize the chosen isotopes by a two-resonance three-color RIS scheme. The ionized atoms are detected after additional mass selection by a TOF analysis.

A simplified level scheme of Pt is shown as an inset in Fig. 1. The first excitation step at 266 nm ($5d^9 6s \ ^3D_3 \rightarrow 5d^9 6p \ ^7_4$), which yields spectroscopic information, is obtained by a single mode injection-locked pulsed dye laser system.¹⁹ The laser pulses delivered by this system are frequency doubled in a potassium dihydrogen phosphate crystal to obtain a 266 nm uv pulse with a spectral width of about 130 MHz. The relative and absolute frequency calibrations are obtained by a Fabry-Perot etalon and an iodine absorption cell. The second and third steps are excited by two pulsed dye lasers pumped by the same excimer laser. The time adjustment between the three ionizing laser pulses is obtained by optical delay lines. An electronic timing box controls the delay between the heating and ionizing lasers, and also provides the starting and deflection pulses for the TOF system. Figure 2 shows the resonance peaks obtained in frequency scans of the even-*A* ¹⁸⁶⁻¹⁹²Pt isotopes.

The IS data obtained for Pt in the 266 nm resonant transition are listed in Table I. The IS (Ref. 20) $\delta v^{A,A'}$ between two isotopes of mass *A* and *A'* is the sum of a mass shift and a field shift (FS). The specific mass shift is assumed to be negligible while the normal mass shift is easily calculated and subtracted. The FS is usually written as $\delta v_{FS}^{A,A'} = F\lambda^{A,A'}$, where $\lambda^{A,A'}$ is a nuclear quantity related to the change in the nuclear charge radius $\delta\langle r^2 \rangle$ via²⁰

$$\lambda^{A,A'} = \delta\langle r^2 \rangle^{A,A'} + (C_2/C_1)\delta\langle r^4 \rangle^{A,A'} + (C_3/C_1)\delta\langle r^6 \rangle^{A,A'} + \dots$$

The electronic factor *F* for the 266 nm transition is obtained from a comparison of the present results with those tabulated by Aufmuth, Heilig, and Steudel²¹ on the stable Pt isotopes for other atomic transitions. This gives us a value of $F = -28 \text{ GHz fm}^{-2}$. We can decompose $\delta\langle r^2 \rangle$ into a spherical term (volume change) and a deformation term (deformation change at constant volume). The small contributions from the higher radial moments contribute differently to the spherical and deformation part and can be taken into account using an expression derived

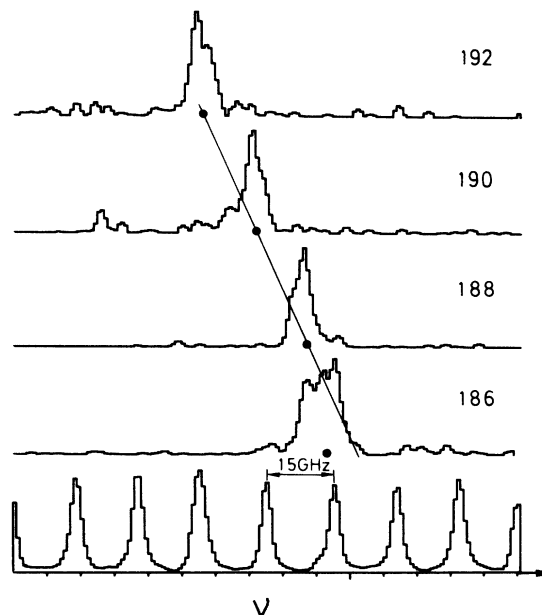


FIG. 2. RIS peaks observed for ¹⁸⁶⁻¹⁹²Pt. With the low production rate of ¹⁸⁶Pt, a reasonable signal could be obtained only by exciting the desorbed atoms close to the substrate: this resulted in a reduced resolution.

TABLE I. Experimental results, deduced nuclear charge radius differences $\delta\langle r^2 \rangle$, and deformation parameter β values.

A	$\delta\nu^{190,A}$ (GHz)	$\delta\langle r^2 \rangle^{190,A}$ (fm ²)	$\delta\langle r^2 \rangle^{A,A+2}$ (fm ²)	$\delta\langle \beta^2 \rangle^{190,A}$	$\langle \beta^2 \rangle^{1/2}$	$\beta[B(E2)]^a$
198	-5.48(31)	0.209(11)	...	-0.0181(10)	0.11 ^b	0.12
196	-3.93(29)	0.150(10)	0.059(5)	-0.0141(9)	0.13	0.14
194	-2.52(26)	0.096(10)	0.054(5)	-0.0098(9)	0.14	0.15
192	-1.19(23)	0.045(8)	0.051(5)	-0.0052(7)	0.16	0.17
190	0	0	0.045(8)	0	0.17	0.17
188	1.05(23)	-0.040(8)	0.040(8)	0.0055(7)	0.19	0.18
186	1.41(36)	-0.053(13)	0.013(11)	0.0134(11)	0.21	0.20

^aReference 7.

^bReference 27.

from the usual two-parameter model of the nuclear shape

$$\lambda^{A,A'} = \delta\langle r^2 \rangle^{A,A'} + x\delta\langle r^2 \rangle_{\text{sph}} + y\delta\langle r^2 \rangle_{\text{def}},$$

where the corrections x and y can be obtained from the liquid drop model.²² Using the values given by the droplet model²³ for $\langle r^2 \rangle_{\text{sph}}$, we extract $\delta\langle r^2 \rangle$ and $\delta\langle r^2 \rangle_{\text{def}}$ from the measured IS. Assuming a pure quadrupole deformation, we obtain the change in the deformation parameter $\delta\langle \beta^2 \rangle$ from

$$\delta\langle r^2 \rangle_{\text{def}} = (5/4\pi)\langle \bar{r}^2 \rangle_{\text{sph}}\delta\langle \beta^2 \rangle.$$

The values of $\delta\langle r^2 \rangle$ and $\delta\langle \beta^2 \rangle$ extracted from the IS data are given in Table I. We note that the change in charge radius $\delta\langle r^2 \rangle^{A,A+2}$ shows a smooth and slow decrease as A is reduced from 198 to 188. However, there is an abrupt decrease in $\delta\langle r^2 \rangle$ between $A=188$ and 186 (see Table I), which supports the evidence from nuclear structure systematics⁷ that a shape transition occurs between ¹⁸⁸Pt and ¹⁸⁶Pt.

The measured $\delta\langle r^2 \rangle$ and deduced deformation can be

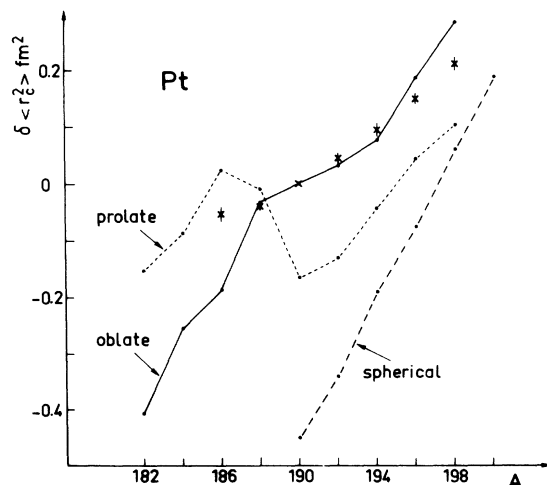


FIG. 3. Change of the mean-square charge radius $\delta\langle r^2 \rangle$ of even- A Pt isotopes. The theoretical curves show the predictions of HF plus BCS calculations (Ref. 24) for oblate and prolate equilibrium solutions. The values found when the nuclei are constrained to spherical shape are also indicated.

compared with theoretical calculations. Several approaches have been used which suggest the nature of the shape transition, and indicate why the observed change in $\delta\langle r^2 \rangle$ and quadrupole deformation parameter β_2 are less dramatic than in the ^{185–186}Hg and ^{186–187}Au transitions. Self-consistent calculations (constrained Hartree-Fock plus BCS method using the S-III Skyrme interaction, assuming axial symmetry) which have already been performed for even- A Os, Pt, and Hg isotopes,²⁴ show two nearly degenerate minima corresponding to oblate and prolate shapes. rms charge radii for both the oblate and prolate equilibrium solutions of ^{184–192}Pt and ¹⁹⁶Pt have been obtained earlier.²⁴ We have extended these calculations to ^{182,194,198,200}Pt. Although such calculations are unable to determine the nuclear charge radii to an accuracy better than 1%–2%, they can reproduce the change of $\delta\langle r^2 \rangle$ very well; for example, comparisons with the deduced radius change for oblate and prolate shapes of the Hg isotopes show nearly perfect agreement.^{1,24} In Fig. 3, experimental and theoretical $\delta\langle r^2 \rangle$ values (relative to ¹⁹⁰Pt) are displayed for all even- A Pt isotopes studied in this work. This shows very good agreement between the

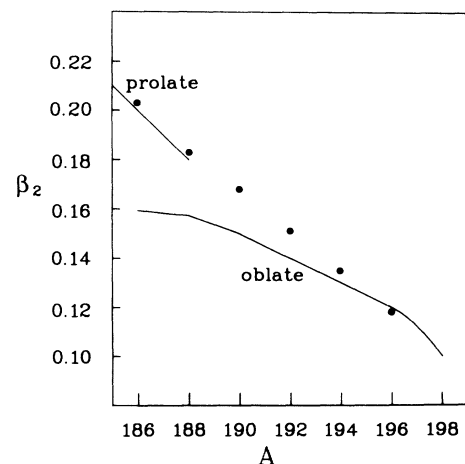


FIG. 4. $\langle \beta^2 \rangle^{1/2}$ values from this work are compared with the theoretical β_2 values of Bengtsson *et al.* (Ref. 11) for prolate and oblate shapes. We have normalized the $\langle \beta^2 \rangle^{1/2}$ value for ¹⁹⁸Pt to 0.10 for this comparison.

oblate theoretical curve and the experimental values from ^{188}Pt to ^{198}Pt . However, for ^{186}Pt , the experimental value deviates markedly from the oblate curve and shifts towards the predicted prolate value, suggesting that a shape transition occurs at this point.

A different approach has been used by Bengtsson *et al.*¹¹ to calculate potential energy surfaces, and to predict the change in β_2 for the even- A Pt isotopes. In that study, a Woods-Saxon potential has been used, with BCS pairing and Strutinsky renormalization. In Fig. 4, the deduced $\langle\beta^2\rangle^{1/2}$ values in the present work are compared with the predicted β_2 values for prolate and oblate shapes. Although in this comparison the transition from oblate to prolate occurs more gradually, with γ softness and asymmetry in ^{188}Pt and ^{190}Pt , the agreement with the predicted β_2 for a prolate ground state in ^{186}Pt is very good. Note

that in this calculation as well, the difference between predicted β_2 values of oblate and prolate shapes is small.

Lattice Hartree-Fock plus BCS calculations for axially asymmetric solutions performed on heavy nuclei²⁵ have also shown that the transition from oblate shape (for ^{196}Pt) to prolate (for $^{186,188}\text{Pt}$) passes through a triaxial shape (for $^{190,192,194}\text{Pt}$).²⁶ The comparison of the present experimental results to the charge radius change extracted from this type of calculation should be very interesting: this extraction is now in progress.

In summary, we believe that the present experiment supports the evidence from nuclear structure studies that a shape transition occurs just above ^{186}Pt . Experiments in progress on the odd- A Pt isotopes should shed further light on the shape changes in this region.

*Present address: Laboratoire Aimé Cotton, Centre National de la Recherche Scientifique II, Orsay, France.

¹J. Bonn *et al.*, Phys. Lett. **38B**, 308 (1972).

²M. Cailliau, J. Letessier, H. Flocard, and P. Quentin, Phys. Lett. **46B**, 11 (1973).

³M. G. Porquet *et al.*, Nucl. Phys. **A411**, 65 (1983).

⁴M. I. Macias-Marqués *et al.*, Nucl. Phys. **A427**, 205 (1984).

⁵K. Wallmeroth *et al.*, Phys. Rev. Lett. **58**, 1516 (1987).

⁶J. K. P. Lee *et al.*, in *Proceedings of the 5th International Conference on Nuclei Far From Stability, Rosseau Lake, 1987*, edited by Ian S. Towner, AIP Conf. Proc. No. 164 (American Institute of Physics, New York, 1988), p. 205.

⁷M. Finger *et al.*, Nucl. Phys. **A188**, 369 (1972).

⁸K. Kumar, Phys. Rev. C **1**, 369 (1970).

⁹G. Hebbinghaus *et al.*, Z. Phys. **A328**, 387 (1987).

¹⁰K. Heyde *et al.*, Phys. Rep. **102**, 291 (1983).

¹¹R. Bengtsson *et al.*, Phys. Lett. **B 183**, 1 (1987).

¹²J. L. Wood, in *Lasers in Nuclear Physics*, Nuclear Science Research Conference Series (Harwood, New York, 1982), Vol. 3, p. 481.

¹³B. Roussière *et al.*, Nucl. Phys. **A 485**, 111 (1988).

¹⁴M. A. Deleplanque *et al.*, J. Phys. (Paris) Colloq. **36**, C5-97 (1975).

¹⁵A. Ben Braham *et al.*, Nucl. Phys. **A332**, 397 (1979).

¹⁶B. E. Gnade, R. W. Fink, and J. L. Wood, Nucl. Phys. **A406**, 29 (1983).

¹⁷B. Roussière, thèse de doctorat d'Etat, Université de Paris-Sud, Orsay, 1986 (unpublished).

¹⁸J. K. P. Lee *et al.*, Nucl. Instrum. Methods **B 34**, 252 (1988).

¹⁹J. Pinard and S. Liberman, Opt. Commun. **20**, 344 (1977).

²⁰E. C. Seltzer, Phys. Rev. **188**, 1916 (1969).

²¹P. Aufmuth, K. Heilig, and A. Steudel, At. Data Nucl. Data Tables **37**, 455 (1987).

²²S. A. Ahmad *et al.*, Z. Phys. **A321**, 35 (1985).

²³W. D. Myers and K. H. Schmidt, Nucl. Phys. **A410**, 61 (1983).

²⁴J. Sauvage-Letessier, P. Quentin, and H. Flocard, Nucl. Phys. **A370**, 231 (1981), and references therein.

²⁵N. Redon *et al.*, Phys. Lett. **B181**, 223 (1986).

²⁶P. Quentin, in *Spectroscopie Nucléaire*, edited by R. Bergère, M. Vergnes, and F. Dykstra (Centre d'Etudes Nucléaires de Saclay, Saclay, 1988), p. 83.

²⁷P. Möller and J. R. Nix, At. Data Nucl. Data Tables **36**, 165 (1981).